

ORIGINAL ARTICLE

Modelling extracellular limitations for mediated versus direct interspecies electron transfer

Tomas Storck¹, Bernardino Virdis^{1,2} and Damien J Batstone¹

¹Advanced Water Management Centre, The University of Queensland, Brisbane, Queensland, Australia and

²Centre for Microbial Electrochemical Systems, The University of Queensland, Brisbane, Queensland, Australia

Interspecies electron transfer (IET) is important for many anaerobic processes, but is critically dependent on mode of transfer. In particular, direct IET (DIET) has been recently proposed as a metabolically advantageous mode compared with mediated IET (MIET) via hydrogen or formate. We analyse relative feasibility of these IET modes by modelling external limitations using a reaction-diffusion-electrochemical approach in a three-dimensional domain. For otherwise identical conditions, external electron transfer rates per cell pair (cp) are considerably higher for formate-MIET ($317 \times 10^3 \text{ e}^- \text{ cp}^{-1} \text{ s}^{-1}$) compared with DIET ($44.9 \times 10^3 \text{ e}^- \text{ cp}^{-1} \text{ s}^{-1}$) or hydrogen-MIET ($5.24 \times 10^3 \text{ e}^- \text{ cp}^{-1} \text{ s}^{-1}$). MIET is limited by the mediator concentration gradient at which reactions are still thermodynamically feasible, whereas DIET is limited through redox cofactor (for example, cytochromes) activation losses. Model outcomes are sensitive to key parameters for external electron transfer including cofactor electron transfer rate constant and redox cofactor area, concentration or count per cell, but formate-MIET is generally more favourable for reasonable parameter ranges. Extending the analysis to multiple cells shows that the size of the network does not strongly influence relative or absolute favourability of IET modes. Similar electron transfer rates for formate-MIET and DIET can be achieved in our case with a slight (0.7 kJ mol^{-1}) thermodynamic advantage for DIET. This indicates that close to thermodynamic feasibility, external limitations can be compensated for by improved metabolic efficiency when using direct electron transfer.

The ISME Journal (2016) 10, 621–631; doi:10.1038/ismej.2015.139; published online 6 November 2015

Introduction

Interspecies electron transfer (IET) is a mechanism whereby different microbial species in a community share reducing equivalents. IET has an important role in bio-electrochemical systems and in other thermodynamically limited processes, such as syntrophic organic acid and ethanol oxidation in anaerobic environments (Boone and Bryant, 1980; Nagarajan *et al.*, 2013).

Mediated IET (MIET) is the most frequently described mode of IET, whereby an electron-carrying compound (mediator) is transported by diffusion from mediator-producing cells to mediator-consuming cells along a concentration gradient. The mediator diffusion rate is limited by the concentration gradient at which oxidation and reduction reactions are thermodynamically feasible (Boone *et al.*, 1989; Batstone *et al.*, 2006).

Hydrogen-MIET has been generally proposed as the dominant transfer mechanism for syntrophic propionate oxidation via acetogenesis and methanogenesis, but alternative IET modes such as formate-MIET have since been suggested, allowing an increased electron transfer rate because of a higher intercellular mediator concentration gradient (Boone *et al.*, 1989; Batstone *et al.*, 2006). Although many methanogenic archaea encode for genes important to formate utilisation, they fail to utilise formate in pure culture (Hedderich and Whitman, 2013), leaving hydrogen as default, presumably the less favourable electron transfer mode.

Direct IET (DIET) has been recently proposed to describe cell–cell electron transfer. DIET is assumed to be analogous to direct extracellular electron transfer, which describes electron transfer between cells and solid-state electron acceptors (for example, iron or manganese oxides, electrodes). Direct extracellular electron transfer research has revolved mainly around studies of bacteria belonging to the genera *Shewanella* and *Geobacter* (Stams *et al.*, 2006), which have proved as highly efficient in engaging with solid extracellular electron acceptors. Cell-to-cell DIET has been observed mainly in defined co-culture IET systems of these organisms

Correspondence: DJ Batstone, Advanced Water Management Centre, The University of Queensland, Level 4, Gehrman Laboratories Building (60), Cooper Road, St Lucia, Brisbane, QLD 4072, Australia.

E-mail: damienb@awmc.uq.edu.au

Received 22 December 2014; revised 15 June 2015; accepted 1 July 2015; published online 6 November 2015

(for example, for *Geobacter metallireducens* and *G. sulfurreducens*) (Summers *et al.*, 2010; Liu *et al.*, 2012; Shrestha *et al.*, 2013), as well as in *Geobacter* dominated mixed-culture performing ethanol oxidation (Morita *et al.*, 2011). Recently, it was shown that DIET can occur in methanogenic systems and between microbial species commonly found in environmental biological aggregates (for example, between *Methanosaeta* and *Geobacter* species) (Rotaru *et al.*, 2014b). Use of DIET over MIET can even enhance the metabolic capability of methanogens such as *Methanosarcina barkeri* to allow methanogenesis simultaneously from CO₂ reduction and acetate cleavage (Rotaru *et al.*, 2014a). Although bacteria belonging to the genus *Shewanella* have been frequently reported to transfer electrons to electrodes or Fe(III) or Mn(IV) oxides, their role in interspecies interaction remains to be reported.

Transcriptomic and proteomic data, together with phenotypes of gene deletion mutants suggested that DIET in syntrophic co-cultures can occur through electrical connections using pili with metallic-like conductivity (Malvankar *et al.*, 2011; Vargas *et al.*, 2013; Malvankar *et al.*, 2014). Outer membrane cytochromes have an important role in extracellular electron transfer to insoluble minerals such as Fe(III) oxides in *Geobacter* (Mehta *et al.*, 2005), as well as in *Shewanella* species (Shi *et al.*, 2009; Okamoto *et al.*, 2011). If electrons during DIET follow a pathway similar to that observed in respiration of Fe(III)/Mn(IV) oxides, then reduced intracellular redox carriers such as nicotinamide adenine dinucleotide would transfer electrons through the extracellular environment via *c*-type cytochromes and conductive pili (Lovley, 2012). At the receiving end of the conductive pili, electrons need to be transferred to the methanogen via another redox complex.

Metabolic modelling of *Geobacter*-mediated ethanol oxidation with sulphate as terminal electron acceptor has suggested that DIET has a metabolic advantage over MIET (hydrogen or formate) (Nagarajan *et al.*, 2013). However, the analysis considered only intracellular metabolism, without taking into account external voltage losses inherent to long-range electron transport. Although DIET does not depend on a mediator to transfer electrons (and is therefore less likely to be limited by diffusion), transport of electrons between the cells through a conductive matrix results in multiple electrochemical losses unique to DIET. These include (1) activation losses (overpotentials) for transfer from a terminal membrane-bound redox complex to the nanowire (and the inverse), (2) electrical resistance of the nanowire and (3) solution resistance caused by migration of ions between the cells. Indirect, secondary limitations may also develop because of development of a pH gradient caused by saline ion migration, and because of accumulation of non-mediator intermediates. A single factor may control, or multiple factors may combine in order to govern feasibility of DIET.

External limitations in nanowire-DIET have not been previously analysed, particularly in relation to well-understood MIET systems. In this work, we propose a mechanistic framework that enables direct assessment of the relative feasibility of DIET and MIET in a thermodynamically restricted syntrophic system (specifically, propionate conversion to acetate and methane).

Model description

Model geometry and components

A three-dimensional transport reaction model has been implemented to calculate the relative feasibility of the three proposed IET modes, hydrogen-MIET, formate-MIET and DIET. Two spherical acetogen and methanogen cells with a diameter of 1 μm each are positioned 5 μm apart and 5 μm from all boundaries of a rectangular domain of size 17 \times 11 \times 11 μm^3 (Figure 1). For DIET, it is assumed that a direct electric connection is made through the formation of 100 nanowires between each cell pair (cp).

The solution consists of primary substrate, carbonate buffer, mediator and products. Owing to the necessity to calculate local pH values, acid dissociation equilibria are included. The chemical components taken into account in the model are therefore protons (H⁺), hydroxide (OH⁻), potassium ion (K⁺), chloride (Cl⁻), propionate (Pro⁻), propionic acid (HPro), bicarbonate (HCO₃⁻), carbon dioxide (CO₂), hydrogen (H₂), formate (For⁻), formic acid (HFor), acetate (Ac⁻), acetic acid (HAc) and methane (CH₄). As the pH was circumneutral, compounds such as carbonate (CO₃²⁻) were found to be very low in concentration, and varied only slightly throughout

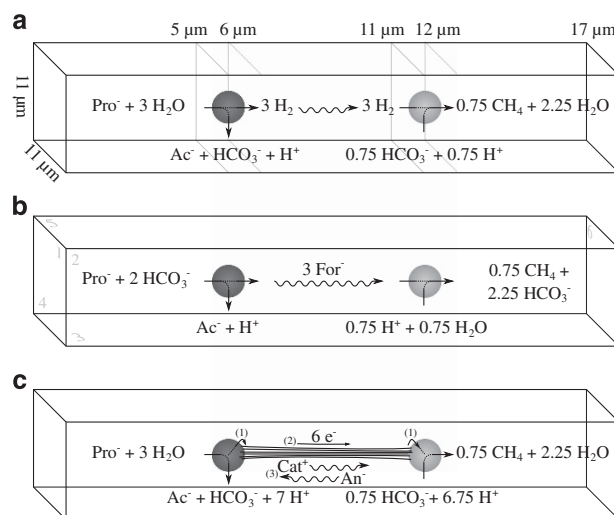


Figure 1 Model geometry, boundary conditions and reactions involved in the three described IET mechanisms: (a) hydrogen-MIET, (b) formate-MIET and (c) DIET. In **b**, on boundaries 1–6 a no-flux condition is set for mediators (H₂, For⁻ and HFor) and fixed concentrations for all other components. Boundary concentration values (*c*_{0,*i*}) are stated in Table 1. A zero-potential is set on boundary 6. In **c**, numbers denote voltage losses for (1) redox factor activation losses, (2) nanowire resistance and (3) migration.

the domain, thereby having negligible effect on the biological reaction feasibility.

Transport of solutes and charge balance

Transport of all chemical compounds in the solution (cells and surroundings) occurs only through diffusion (introducing diffusion coefficient D) and migration (charge z and migration potential field Φ_{mig}), as described by the steady-state Nernst–Planck equations:

$$\nabla \cdot J_i = r_i \quad \text{with flux} \quad J_i = -D_i \nabla c_i - \frac{z_i D_i F}{RT} c_i \nabla \Phi_{\text{mig}} \quad (1a)$$

with reaction rates r_i calculated as described in the next section, the unknowns in the system are the 14 concentrations c_i and the potential field gradient $\nabla \Phi_{\text{mig}}$ (15 unknowns per control element). Given Equation (1a) is applied for each component i (14 equations), the system is fully defined by setting the potassium ion concentration to satisfy the electroneutrality condition:

$$c_{\text{K}^+} = - \sum_{i \neq \text{K}^+} z_i c_i \quad (1b)$$

In order to determine IET rates based only on cell metabolism, no-flux boundary conditions ($-\mathbf{n} \cdot J_i = 0$, where \mathbf{n} is the normal vector) for the mediator and fixed concentrations ($c_i = c_{0,i}$) for all compounds are set at all domain boundaries (Figure 1b). All boundaries are electrically insulated ($-\mathbf{n} \cdot F \sum_i z_i J_i = 0$), except one arbitrary face of the domain for which the potential Φ_{mig} is set to a reference value ($\Phi_{\text{mig}} = 0 \text{ V}$) to allow calculation of Φ_{mig} from $\nabla \Phi_{\text{mig}}$. Default parameter values are listed in Table 1 and Supplementary Table 1.

Reaction rates

For each compound i , the net volume-specific rate r_i in Equation (1a) includes contributions from biological conversions $r_{B,i}$ and acid dissociation $r_{A,i}$ (Batstone *et al.*, 2002). Dissociation reactions occur throughout the entire domain, whereas biological conversions only take place in the cells. The net biological contributions, $r_{B,i} = \sum_j \nu_{ji} r_{X,j}$, are calculated with cell reaction rate $r_{X,j}$ and stoichiometry coefficients ν_{ji} specific for reactions occurring in each cell type as given in Figure 1. Owing to the cellular scale and thermodynamic restrictions, cell reaction rate can be completely regulated by a thermodynamic inhibition function that incorporates substrate, intermediate and product concentrations, such that empirical rate functions like the Monod equation (Batstone *et al.*, 2006) can be omitted. The cell uptake rate (basis 1 mol propionate, 3 mol mediator, 6 mol e^- equivalents) is given by the maximum rate (r_X^{max}), limited by inhibition factors

$f_{\text{inh},j}$ (constrained to $0 < f_{\text{inh},j} < 1$):

$$r_{X,j} = \begin{cases} r_X^{\text{max}} f_{\text{inh},\text{MIET},j} & \text{for MIET} \\ r_X^{\text{max}} f_{\text{inh},\text{DIET},jk} & \text{for DIET, two-cell system} \end{cases} \quad (2a)$$

$$r_{X,j} = \begin{cases} r_X^{\text{max}} f_{\text{inh},\text{MIET},j} & \text{for MIET} \\ r_X^{\text{max}} f_{\text{inh},\text{DIET},jk} & \text{for DIET, two-cell system} \end{cases} \quad (2b)$$

For MIET, the only extracellular factor considered to limit the rate is thermodynamic inhibition:

$$f_{\text{inh},\text{MIET},j} = 1 - \exp\left(\left(\Delta G'_{r,j} - \Delta G'_{\text{diss}}\right)/RT\right) \quad (3)$$

Equation (3) is equivalent to previously described inhibition functions (Hoh and Cord-Ruwisch, 1996; Batstone *et al.*, 2006), but with the inclusion of a Gibbs free energy dissipation term ($\Delta G'_{\text{diss}}$) that defines the threshold energy required for cell anabolism, catabolism and maintenance. By using $f_{\text{inh},\text{MIET},j}$, the cell is limited only by the Gibbs free energy available for electron transport ($\Delta G'_{r,j} - \Delta G'_{\text{diss}}$) generated by the catabolic reaction considered in each cell. $\Delta G'_{r,j}$ is a function of the surface-averaged concentration $\langle c_i \rangle_j$ (in mol l^{-1} , for all aqueous solutions) or partial pressure (in bar, for gases H_2 and CH_4 only) of reactants and products i for cell j , expressed as:

$$\Delta G'_{r,j} = \Delta G^0_{r,j} + RT \ln \left(\prod_{i \neq \text{H}_2, \text{CH}_4} \left\langle \frac{c_i}{c_{\text{ref}}} \right\rangle_j^{\nu_{ji}} \prod_{i = \text{H}_2, \text{CH}_4} \left\langle \frac{p_i}{p_{\text{ref}}} \right\rangle_j^{\nu_{ji}} \right) \quad (4)$$

Here, c_{ref} and p_{ref} are the reference concentration and pressure, 1 mol l^{-1} and 1 bar, respectively. Through Equations (2)–(4), $r_{X,j}$ is completely regulated by $\langle c_i \rangle_j^{\nu_{ji}}$, $\langle p_i \rangle_j^{\nu_{ji}}$ and $\Delta G^0_{r,j}$. With r_X^{max} sufficiently high, an increase in r_X^{max} is compensated for by a small decrease in $f_{\text{inh},\text{MIET},j}$ via small changes in $\langle c_i \rangle_j^{\nu_{ji}}$ and $\langle p_i \rangle_j^{\nu_{ji}}$. r_X^{max} can therefore be set to an arbitrarily high value so that reactions proceed at their thermodynamic limit ($\Delta G'_{r,j} - \Delta G'_{\text{diss}}$ approaches 0). Owing to low mediator concentrations and the reaction stoichiometry, Equation (4) is dominated by the mediator term ($\langle p_{\text{H}_2} \rangle_j^{\nu_{j,\text{H}_2}}$ or $\langle c_{\text{For}^-} \rangle_j^{\nu_{j,\text{For}^-}}$).

As stated above, $r_{X,j}$ is not governed by a kinetic function but it operates at the highest rate that is thermodynamically possible. The critical parameter is the Gibbs free energy required for dissipation ($\Delta G'_{\text{diss}}$), which has been estimated to be between -15 and -25 kJ mol^{-1} substrate (Stams and Plugge, 2009) for propionate acetogenesis/methanogenesis. Other methods generally suggest higher values (for example, > -100 kJ mol^{-1} ; Heijnen and Kleerebezem (2010); see Supplementary Table 2), suggesting a highly efficient metabolism for propionate oxidation. Note that a larger (more negative) $\Delta G'_{\text{diss}}$ will result in a lower rate, although both MIET and DIET will be uniformly impacted.

Table 1 Default model parameter values

Symbol	Unit	Description	Default value	Reference and notes
<i>Geometry</i>				
A_{cell}	m ²	Surface area of cell	3.14×10^{-12}	Calculated from d_{cell}
d_{cell}	m	Diameter cell (acetogen, methanogen)	1.00×10^{-6}	
<i>Concentrations</i>				
c_0	mol m ⁻³	Fixed boundary concentration		
		Propionic acid	7.41×10^{-3}	
		Propionate	1.00	
		Acetic acid	5.75×10^{-3}	
		Acetate	1.00	
		Carbon dioxide	22.39	
		Bicarbonate	100	
		Methane	0.1438	Calculated from $p_{0,\text{CH}_4} = 0.1$ bar
		Proton	1.00×10^{-4}	pH 7
		Hydroxide	1.01×10^{-4}	
		Chloride	1000	
		Potassium ion	1102	Closes charge balance
<i>Thermodynamics and electrochemical</i>				
$\Delta G'_{\text{diss}}$	J mol ⁻¹	ΔG diss. through catabolism, anabolism, maintenance	-15.2×10^3	Boone and Bryant (1980)
V_{diss}	V	V dissipated through catabolism, anabolism, maintenance	52.51×10^{-3}	Calculated as $-2\Delta G'_{\text{diss}}/6F$
<i>Butler–Volmer (DIET only)</i>				
$A_{\text{act,cell}}$	m ²	Total area for redox cofactor activation for any cell	3.14×10^{-13}	10% of A_{cell} , Supplementary Table 2
c_{act}^s	mol m ⁻²	Redox cofactor surface concentration	5.29×10^{-9}	Supplementary Table 2
k_0	s ⁻¹	Standard redox cofactor activation rate constant	6000	Supplementary Table 3, Ly et al. (2013)
$N_{\text{act},j}$	—	Number of redox cofactors per nanowire for cell j		$N_{\text{act,cell}}/N_{\text{nw},j}$
$N_{\text{act,cell}}$	—	Number of redox cofactors per cell	1.0×10^4	Lower et al. (2007)
β	—	Symmetry factor	0.5	
<i>Ohm's law (DIET only)</i>				
A_{nw}	m ²	Cross-sectional area of a single nanowire	1.26×10^{-17}	Calculated from d_{nw}
d_{nw}	m	Diameter of single nanowire	4.00×10^{-9}	Malvankar et al. (2011)
L_{nw}	m	Length of single nanowire	5.0×10^{-6}	Default value for cell pair model only
$N_{\text{nw},j}$	—	Total number of nanowires connected to cell j		(Number of connected cells k) $\times N_{\text{nw,pair}}$
$N_{\text{nw,pair}}$	—	Number of nanowires formed per cell pair	100	
ρ_{nw}	Ω m	Electrical resistivity of nanowire	1.0	Malvankar et al. (2011)

Abbreviation: DIET, direct interspecies electron transfer. The complete default parameter set with nomenclature is available in supplementary material as Supplementary Table 1.

Applying our model specifically to a propionate grown co-culture of *Syntrophobacter wolinii* and *Methanospirillum hungatei* (both capable of formate-MIET) growing on propionate (Boone and Bryant, 1980) and applying a growth yield ($Y_{S/X}$) of 0.15 Cmol mol⁻¹ propionate, based on the observed growth rate and applied substrate concentrations (Boone and Bryant, 1980), we estimate $\Delta G'_{\text{diss}} = -15.2$ kJ mol⁻¹ for both cell types (see Supplementary Figure 1). This value is applied to DIET and MIET. Asymmetric maintenance is also possible because of the methanogen needing to utilise reverse electron transport (Stams and Plugge, 2009) and this is also addressed later in the article.

The only difference between implementations for DIET and MIET is in the direct electron transfer component. In DIET, electrons are transferred between acetogen and methanogen through a conductive system driven by a voltage $V_{\text{net},jk}$ between the two cells j and k . Electrons are produced through propionate metabolism by an oxidising cell, and then transferred to the reducing cells for carbon dioxide conversion (see Figure 1c). Unlike with MIET, where

the feasibility of the reaction is determined by the cell environment, the feasibility of the DIET reaction pair is determined on its paired basis. The net voltage available ($V_{\text{net},jk}$) in the two-cell system is equal to the voltage available from the reaction given in Figure 1c ($V_{r,jk}$) minus DIET-specific voltage losses for electron transfer between membrane-bound redox cofactors and nanowire (activation losses) at both cells j and k , nanowire resistance, and ion migration in the solution, as depicted by Equation (5):

$$V_{\text{net},jk} = V_{r,jk} - \eta_{\text{act},j} - \eta_{\text{act},k} - \eta_{\text{nw},jk} - \eta_{\text{mig},jk} \quad (5)$$

The voltages in Equation (5), $V_{\text{net},jk}$ and V_r , relate to Gibbs free energy changes via $V = -\Delta G'/(F\nu_{e^-})$ (where $\nu_{e^-} = 6$, the number of electrons involved in the catabolic half reaction), so that $V_{r,jk}$ is calculated via the surface-averaged concentrations (using Equation (4) and $\Delta G'_{r,jk} = \Delta G'_{r,j} + \Delta G'_{r,k}$). We found that because no mediator is involved for DIET, none of the terms $\langle c_i \rangle_j^{\nu_{ij}}$ and $\langle p_i \rangle_j^{\nu_{ij}}$ changes significantly with IET rate and as a result the voltage available from reaction is constant for all reported DIET rates

($V_{r,jk} = 52.93$ mV). Whereas MIET is regulated via the energy made available by the catabolic reaction ($\Delta G'_{r,j}$), DIET is controlled via the external electron transfer voltage losses (η). As voltages V_{jk} and voltage losses η_{jk} in Equation (5) are defined for the oxidising-reducing cell pair, the values observed by cell j are identical to those observed by its partner k (that is, $V_{jk} = V_{kj}$ and $\eta_{jk} = \eta_{kj}$).

The electron transfer rate is limited by an inhibition function governed by the net and dissipation voltage:

$$f_{\text{inh,DIET},jk} = 1 - \exp(-Fv_e(V_{\text{net},jk} - V_{\text{diss}})/RT) \quad (6)$$

There are two differences between the model for MIET and DIET. First, additional losses specific for DIET are taken into account (Equation (5)) and second, inhibition for cell j (Equation (6)) depends also directly on cell k ($V_{\text{net},jk} = V_{\text{net},kj}$, therefore $f_{\text{inh,DIET},jk} = f_{\text{inh,DIET},kj}$). Although Equation (6) is expressed as voltage rather than free energy as in Equation (3), the two regulation functions (3) and (6) are completely analogous as seen through the voltage–Gibbs free energy relation above.

The dissipation voltage (V_{diss}) can be calculated directly from the voltage–Gibbs relation and $\Delta G'_{\text{diss}}$, yielding $V_{\text{diss}} = 52.51$ mV for any cell pair.

Cell conversion rates ($r_{X,j}$) are volume specific and are referenced to the primary substrate. In order to express the rate per cell, the cell-specific electron transfer rate has been calculated as $\text{rate}_{\text{IET},j} = r_{X,j} \pi d_{\text{cell}}^2 N_A$ (where N_A is Avagadro's number and 6 mol electrons are transferred per mol propionate consumed), with unit $e^- s^{-1}$.

Redox cofactor activation losses

Activation losses occur each time an electron is transferred from the electron carrier associated with the membrane to the nanowire or *vice versa*. Both of these voltage losses ($\eta_{\text{act},j}$ and $\eta_{\text{act},k}$; (1) in Figure 1c) are calculated using the Butler–Volmer equation assuming a one-step, single-electron transfer process. The total current between the cells (I_{jk}) is the same in the electron-producing and -consuming cells ($I_{jk} = I_{kj} = \text{rate}_{\text{IET},jk} F/N_A$), and this current is distributed evenly over the nanowires connecting the cells (analogous to an electrical circuit in parallel). The Butler–Volmer equation used to calculate the activation voltage loss ($\eta_{\text{act},j}$) is as shown in Equation (7) (Bard and Faulkner, 1980; Noren and Hoffman, 2005):

$$I_{jk}/N_{\text{nw,pair}} = FA_{\text{act},j} k_0 c_{\text{act}}^s \left(e^{(1-\beta)(F/RT)\eta_{\text{act},j}} - e^{-\beta(F/RT)\eta_{\text{act},j}} \right) \quad (7)$$

The number of nanowires present between the cell pair ($N_{\text{nw,pair}}$), symmetry factor (β), cofactor electron transfer rate constant (k_0) and activation cofactor concentration (c_{act}^s) have been taken as the same for electron-producing and -consuming cells. Given that the redox cofactor surface area available for activation ($A_{\text{act},j}$) is calculated as described below, $\eta_{\text{act},j}$ remains as the only unknown. The

Butler–Volmer equation can therefore be solved implicitly to determine voltage losses $\eta_{\text{act},j}$ and $\eta_{\text{act},k}$ at which the current will be at its maximum.

To determine the total redox cofactor surface area per cell ($A_{\text{act,cell}}$), it was estimated that in total 10% of the cell surface area is available to transfer electrons to the nanowires, regardless of the number of nanowires. This estimate considers 10^4 redox cofactors ($N_{\text{act},j} = 10^4$) present on the cell surface of a *Shewanella* cell (Lower *et al.*, 2007) and a redox cofactor diameter between 5 and 8 nm in diameter (Wigginton *et al.*, 2007), using which the cytochrome coverage is calculated as around between 6% and 16% (Supplementary Table 3). These values match well to estimates made by Okamoto *et al.* (2009). The available redox cofactor area per connection is calculated assuming that the total redox cofactor area available is distributed evenly over all nanowires connected to cell j ($A_{\text{act},j} = A_{\text{act,cell}}/N_{\text{nw},j}$). In a two-cell system, this simplifies to $A_{\text{act},j} = A_{\text{act},k}$, such that activation losses are the same at both cells ($\eta_{\text{act},j} = \eta_{\text{act},k}$).

The cofactor electron transfer rate constant k_0 for redox cofactor–nanowire transfer is not readily available in literature. However, redox cofactor–electrode electron transfer rate constants have been reported. The heterogeneous rate constant for outer membrane cytochromes on *Shewanella* has been calculated as $150 s^{-1}$ (Okamoto *et al.*, 2009). Using the redox cofactor concentration derived from $N_{\text{act,cell}}$, the surface concentration (c_{act}^s) is estimated to be 5.29×10^{-9} mol m^{-2} . This matches well with the experimentally observed exchange current density (Bowden *et al.*, 1982; Reed and Hawkrige, 1987), as shown in Supplementary Table 4. Rates for electron transfer within a biofilm have been estimated to be 40 times faster than for transfer between biofilm and electrode (Ly *et al.*, 2013). Therefore, for both the acetogen and methanogen, we consider k_0 as equal to $6000 s^{-1}$. Further research could provide insight to the correctness of this estimate. As no direct measurements have been done on Butler–Volmer parameters for system modelled in our work, we also provide a sensitivity assessment to test a range of parameters.

Nanowire ohmic losses

Ohmic conductivity for the nanowire is assumed because of recent experimental support (Malvankar *et al.*, 2014) and as experimentally observed parameters can be found in literature (El-Naggar *et al.*, 2010; Malvankar *et al.*, 2011). The voltage loss because of nanowire resistance is calculated using Ohm's law, expressed for this system as:

$$\begin{aligned} \eta_{\text{nw},jk} &= R_{\text{nw},jk} I_{jk} / N_{\text{nw,pair}} \\ &= \rho_{\text{nw}} L_{\text{nw},jk} I_{jk} / N_{\text{nw,pair}} A_{\text{nw}} \end{aligned} \quad (8)$$

which is function of the IET rate, resistivity (ρ_{nw}), nanowire length ($L_{\text{nw},jk}$) and nanowire cross-sectional area (A_{nw}). Parameters for nanowire losses are

taken from measurements performed on *Geobacter sulfurreducens*. The nanowire length is set as the interspecies distance, 5 μm (Figure 1). The nanowire diameter is $d_{\text{nw}}=4$ nm and the electrical resistivity $\rho_{\text{nw}}=1$ Ω m (Malvankar *et al.*, 2011).

Migration losses

The voltage loss because of extracellular ion migration in DIET, $\eta_{\text{mig},jk}$, is related to an extracellular electric field (E) formed in the medium as a result of ion transport, Equations (1a and b). This electric field causes a potential field (related via $E=-\nabla\Phi$) resulting in an overall voltage loss $\eta_{\text{mig},jk}$. A potential field is implicitly calculated in the modelling package used (and has been separately verified by calculation), from which $\eta_{\text{mig},jk}$ is calculated as the difference between the average value of Φ_{mig} at the surfaces of methanogen and acetogen cells ($\eta_{\text{mig},jk} = |\langle \Phi_{\text{mig}} \rangle_k - \langle \Phi_{\text{mig}} \rangle_j|$, the absolute value is taken such that $\eta_{\text{mig},jk} = \eta_{\text{mig},kj} > 0$ in Equation (5)). This loss is only relevant for DIET because electrons are transferred separate from the ions.

Implementation of for a multicellular system

The MIET model can be directly implemented in a multicellular system without modification. When applying the DIET model to a larger cell community, the key complication is sharing of electrons between multiple pairs of donors and acceptors while maintaining a closed electron balance for all cell pairs. We propose here a method using an electron balancing factor, $f_{\text{bal},jk}$, for each cell in a pair that limits the rate of faster reacting cells to the rate of its connected partners. The DIET rate (Equation (2b)) can be rewritten for a multicellular system:

$$r_{X,j} = \sum_k r_{X,jk} = r_X^{\text{max}} \sum_k \left(f_{\text{inh,DIET},jk} f_{\text{bal},jk} \right) \quad (9)$$

for DIET, multicellular system

$f_{\text{bal},jk}$ is a limiting factor ($0 \leq \sum_k f_{\text{bal},jk} \leq 1$) introduced to satisfy the electron balance in the system and is needed when a cell forms connections with multiple other cells. When modelling a single-cell pair with the same r_X^{max} , rates are always balanced ($\sum_k f_{\text{bal},jk} = \sum_j f_{\text{bal},kj} = 1$) because the inhibition factor is the same for both cells (all terms in Equation (6) are the same for j and k , so $f_{\text{inh,DIET},jk} = f_{\text{inh,DIET},kj}$), thereby reducing multicellular DIET rate Equation (9) to two-cell system DIET rate Equation (2b).

The reason an extra factor $f_{\text{bal},jk}$ must be introduced for a multicellular system is related to the redox cofactor area. As stated before, it is assumed that the total area of membrane-bound redox proteins $A_{\text{act,cell}}$ is the same for all cells and is shared evenly among the connected nanowires. For the multicellular system, one cell j can form a different number of nanowires than cell k , so that the redox cofactor area available to each nanowire connected to cell j , $A_{\text{act},j}$, is no longer equal to $A_{\text{act},k}$. The activation loss for

j can thereby be limited in a different way than for cell k that is connected to a different number of cells ($N_{\text{nw},j} \neq N_{\text{nw},k}$, so $\eta_{\text{act},j} \neq \eta_{\text{act},k}$ as per Equation (7)), resulting in a different set of inhibition factors for cell j , k and their respective partners, consecutively requiring an extra rate balancing factor $f_{\text{bal},jk} \neq f_{\text{bal},kj}$ to close the electron conservation balance. $f_{\text{bal},jk}$ is calculated for all cells and neighbours by maximising the total IET rate.

In order to investigate how electrons are shared according to the method described here and how sharing affects the total IET rate, a case study is set up involving 12 acetogens and 12 methanogens distributed randomly in a $30 \times 30 \times 30$ μm^3 domain. An average interspecies distance of 5 μm between a cell and its closest partner is enforced and 100 nanowires are taken to be present between an acetogen and each methanogen in a 10 μm radius (that is, $N_{\text{nw,pair}}$ remains 100, but $N_{\text{nw},j} = \sum_k N_{\text{nw,cell}}$ can exceed 100).

Implementation

Both two-cell and multicellular models were implemented in COMSOL Multiphysics (COMSOL 4.4, COMSOL Inc., Burlington, MA, USA) using the Nernst–Planck equations module. Two Global ODEs and DAEs modules are set up and solved in parallel to determine the voltage losses for the Butler–Volmer and Ohm’s law equations. For the multicellular model, the model geometry was defined in MATLAB and transferred via LiveLink (MATLAB 2014a, MathWorks, Natick, MA, USA). $f_{\text{bal},jk}$ is determined by minimising $(\sum_j \text{rate}_{\text{IET},j})^{-1}$ using a SNOPT algorithm optimiser (Gill *et al.*, 2005). Model code can be provided by the corresponding author on request.

Results and Discussion

Two-cell system

Results for single-cell pair simulations show that MIET is controlled by hydrogen and formate/formic acid diffusion. The concentration along the centre of the domain changes by <0.01% of the mean concentration for all components except hydrogen, formate and formic acid (Figure 2a). DIET rates are controlled by activation losses (93% of total voltage losses, see Figure 2b), whereas migration losses and diffusion limitation are insignificant ($\eta_{\text{mig}} \ll 1\%$ total voltage losses and the overall relative concentration differences for all components <0.01%). Formate-MIET (317×10^3 $\text{e}^- \text{cp}^{-1} \text{s}^{-1}$, Figure 2c) is thermodynamically the most favourable IET mode, with the DIET rate 1 order of magnitude (44.9×10^3 $\text{e}^- \text{cp}^{-1} \text{s}^{-1}$) and the hydrogen-MIET rate 2 orders of magnitude lower (5.24×10^3 $\text{e}^- \text{cp}^{-1} \text{s}^{-1}$). Thus, considering external factors and with the baseline parameters chosen, DIET is more favourable than hydrogen-MIET, but substantially less favourable than formate-MIET. All values are well below the maximum biomass-specific electron transfer rate identified by Heijnen and

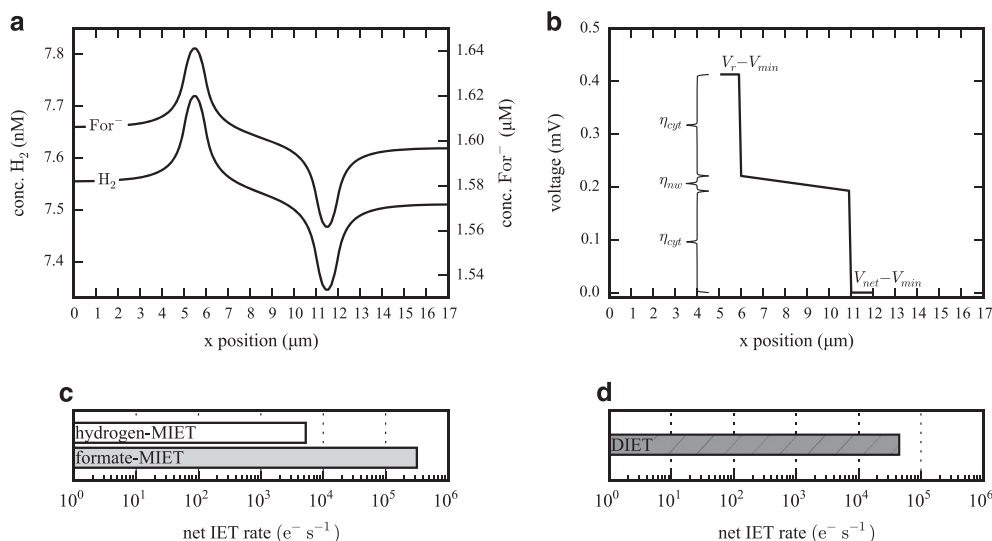


Figure 2 (a) Mediator profiles along the centre of the domain (x axis at $L_x/2$, $L_z/2$) for formate- and hydrogen-MIET, for the default parameter set. (b) DIET voltage and losses along the nanowire, default parameter set. Note that η_{mig} is negligible compared with other losses. (c, d) Net IET rates for MIET and DIET, respectively, default parameter set.

Kleerebezem (2010), corresponding to 10^7 e⁻ s⁻¹ (see Supplementary Table 5).

The main reason formate-MIET allows a greater transfer rate than hydrogen-MIET (Figure 2c) is because it allows a larger concentration gradient while maintaining feasible thermodynamics (Figure 2a), despite the higher diffusion coefficient of hydrogen. This aligns well with previous analysis (Boone *et al.*, 1989; Batstone *et al.*, 2006).

DIET activation losses are strongly dependent on multiple parameters, which have limited literature support, likely the most arguable value being the cofactor electron transfer rate constant (k_0). Reducing k_0 by a factor 10 (for example, if redox cofactor-nanowire transfer is not 40 but only 4 times faster than redox cofactor-electrode, or if k_0 is 10-fold lower than reported in Okamoto *et al.*, 2009) makes activation voltage losses even more dominant (99.2% of total voltage losses) and lowers the feasibility for DIET to a rate lower than hydrogen-MIET (Figure 3, case 2). Doubling the cofactor electron transfer rate constant almost doubles the IET rate, with activation losses responsible for 87% of the total voltage losses. It is not until k_0 is increased 10-fold that redox cofactor activation is no longer the only governing loss (57% of the total voltage losses, the remaining 43% attributed to Ohmic losses in the nanowire) and that the DIET rate approaches the formate-MIET rate (to 90%). From Equation (7) it can be seen that the same effects can be obtained by varying $A_{act,cell}$ or c_{act}^s with the same factor instead of k_0 . An increase of $A_{act,cell}$ could be justified by assuming a different larger size of the redox cofactor (for example, Edwards *et al.*, 2014), a decrease by considering the cell surface not facing the other cell is unlikely to be used. Similarly, an increase in c_{act}^s is possible if redox cofactors are preferentially located where

electron transfer to nanowires occurs, instead of homogeneously distributed over the cell surface.

The amount of cytochromes on the cell surface ($N_{act,cell}$) governs both c_{act}^s and $A_{act,cell}$ and will therefore have an even stronger effect on the DIET rate than the same relative change in k_0 , although the range through which $N_{act,cell}$ can be varied is smaller (for example, a 10-fold increase in would result in an unrealistic 100% redox cofactor coverage). Reducing $N_{act,cell}$ by a factor 5 makes DIET less than half as feasible as hydrogen-MIET (Figure 3, case 3), whereas increasing $N_{act,cell}$ by a factor 5 makes DIET thermodynamically more feasible than formate-MIET.

A small fraction of the total voltage losses for the default parameters is due to Ohmic losses in the nanowire. The resistivity (ρ_{nw}) used to determine Ohmic losses was measured for a biofilm (Malvankar *et al.*, 2011), which means that the actual resistivity of an individual nanowire could be smaller. Reducing ρ_{nw} by 2 orders of magnitude (for example, to the resistivity reported for individual nanowires in *Shewanella oneidensis*; El-Naggar *et al.*, 2010) causes a small increase in the DIET rate (Figure 3, case 4), as the system is completely dominated by activation losses (99.9% of total voltage losses). Alternative nanowire conductivity models, such as electron hopping between redox components aligned along membrane vesicles as recently suggested to account for conduction in *Shewanella oneidensis* nanowires (Pirbadian *et al.*, 2014), could be implemented in the model described here by considering a series of redox cofactor activation steps along the nanowire. The activation energy for a single step as calculated here, although, indicates that the standard activation rate constant k_0 for cofactor-cofactor electron transfer will need to be orders of magnitude higher than the k_0 used in this model for cytochrome hopping to be thermodynamically feasible.

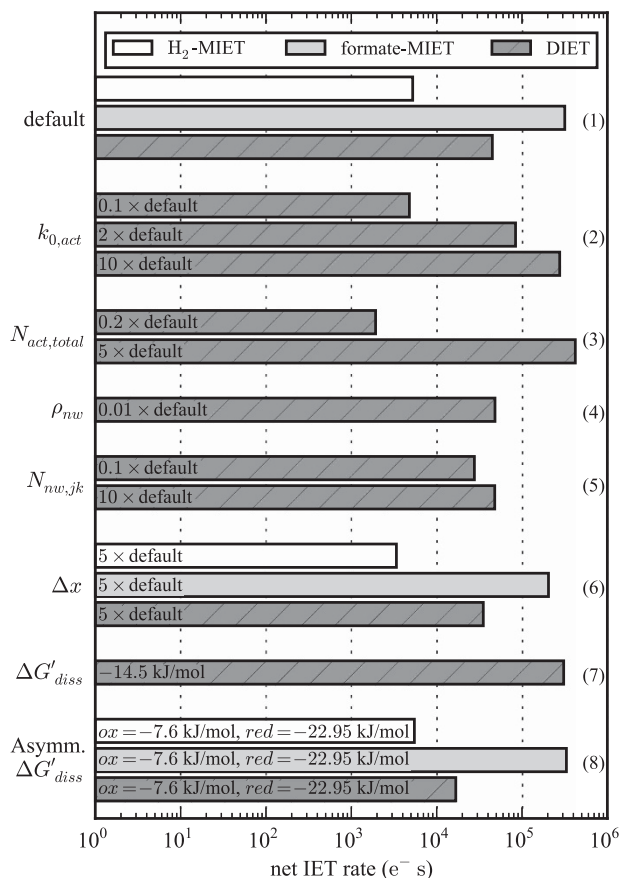


Figure 3 Sensitivity analysis for cell pair IET rates. The numbers on the right-hand side indicate different parameter sensitivity studies (cases) and are referred to in the text. Note that case 1 shows the same data as Figures 2c and d.

The number of nanowires formed per cell pair ($N_{nw,pair}$) has a strong effect on the Ohmic loss (affecting the current per nanowire, $I_{jk}/N_{nw,pair}$, via Equation (8)) but no effect on activation losses (changes to the current per nanowire and $A_{act,j}$ cancel out), therefore a 10-fold increase in $N_{nw,pair}$ will have the same effect as a 10-fold decrease in ρ_{nw} . The range through which $N_{nw,pair}$ can be varied is different from the range for ρ_{nw} , however. The number of nanowires could be an order of magnitude lower or higher than the default value of 100. If 10 nanowires are formed per cell pair, the DIET rate changes to 60% of the original value, whereas 1000 nanowires per cell pair would result in an IET rate 107% of the default rate (Figure 3, case 5) as the system is fully dominated by activation losses.

Increasing interspecies distance (Δx) to 25 μm limits the DIET rate by increasing Ohmic losses but does not affect the redox cofactor activation losses, whereas for MIET the concentration gradient and thereby the diffusion flux is lowered. The model shows that a five times larger Δx attenuates MIET more than DIET, as DIET activation losses remain dominant (75% of the total voltage losses), resulting in a rate 80% of the original rate, whereas both MIET rates drop to 65% of the original rate (Figure 3, case 6).

This suggests DIET may be a thermodynamically more feasible alternative to MIET for disperse communities limited by diffusion, which is contrary to experimental observations where nanowire-DIET is commonly observed in dense aggregates (Summers *et al.*, 2010; Rotaru *et al.*, 2014), possibly indicating that co-evolution and co-metabolism are more important than external limitations in this system. We also note that use of non-organic conductive elements such as activated carbon (Liu *et al.*, 2012) and magnetite (Cruz Viggi *et al.*, 2014) could reduce resistivity, and leave only activation losses (although these will likely be increased), possibly making long-range transport even more feasible.

The combined effect of uncertainties in these DIET parameters were taken into account through a Monte-Carlo analysis with a coarse mesh (1000 simulations; coarse mesh affects DIET rates $\ll 1\%$). The median rate observed is $11.9 \times 10^3 \text{ e}^- \text{cp}^{-1} \text{ s}^{-1}$, showing that combined uncertainties are likely to further decrease the actual DIET rate. However, the 95% prediction interval contains both default MIET rates, emphasising the importance of obtaining more accurate experimental estimates of parameters involved in DIET. A histogram showing the distribution of IET rates is given in Supplementary Figure 2.

The work done here only considers external limitations, and does not consider that there are energetic losses involved in translation of electrons to an electron mediator as assessed by (Nagarajan *et al.*, 2013). Metabolic modelling indicated that the cell metabolism for DIET is more efficient than for MIET, justifying a less negative value for $\Delta G'_{diss}$ (resulting in a smaller V_{diss}). Comparing formate-MIET at a $\Delta G'_{diss} = -15.2 \text{ kJ mol}^{-1}$ per cell to DIET at a slightly less negative $\Delta G'_{diss}$ values (for example, $-14.5 \text{ kJ mol}^{-1}$, see Figure 3, case 7), suggests that for IET rates reported in this work (10^3 – $10^5 \text{ e}^- \text{cp}^{-1} \text{ s}^{-1}$) a slightly more efficient metabolism for DIET is enough for the rate to match the formate-MIET rate. This result is important because it suggests that comparative external electron transfer feasibility (sometimes resulting in order of magnitude different rates) can be compensated for by very slight advantages in cellular metabolism.

The value for $\Delta G'_{diss}$ is assumed to be the same for the acetogen and methanogen in the default case. Methanogens are expected to have higher energy dissipation than acetogens because of the reverse electron transfer process required to allow reduction of CO_2 to biomass. It has been suggested that the $\Delta G'_{diss}$ for the methanogen is at least three times higher than for the acetogen (Heijnen and Kleerebezem, 2010). Given this ratio and recalibrating for the same default formate-MIET transfer rate, $\Delta G'_{diss}$ is set to be -7.6 kJ mol^{-1} for the acetogen and $-22.95 \text{ kJ mol}^{-1}$ for the methanogen. It was found that while both MIET rates achieve the same rate as in the default case, the DIET rate is lowered to less

than 40% of the original value (Figure 3, case 8). This shows that the asymmetric energy dissipation values of the acetogen and methanogen affect the thermodynamic feasibility and that the relative DIET feasibility is likely to be further impeded.

Multicellular system

The multicellular system was implemented to demonstrate application of the two-cell principles in a multicellular system, and identify whether a three-dimensional field with multiple sources and sinks would result in a different overall transfer rate. Experimentally observed systems analogous to this model include *Geobacter metallireducens*/*Methanosaeta harundinacea* (Rotaru et al., 2014b) and *Geobacter metallireducens*/*Methanosarcina barkeri* (Rotaru et al., 2014), both of which degrade ethanol to methane, a conversion that is analogous to propionate oxidation but with more favourable thermodynamics.

Results are shown in Figure 4 and represent simultaneously electron transfer rate between cells (coloured links), as well as overall migration potential field in two planes (coloured sections). Although the migration potential field and the resulting losses $\eta_{mig,jk}$ are not limiting electron transfer, it does indicate that the potential field is governed mainly by interacting pairs. The results indicate that a multicellular system achieves

slightly lower DIET rates per cell (on average 15% lower, $r_{x,j} = 38.2 \times 10^3$ versus $44.9 \times 10^3 \text{ e}^- \text{ s}^{-1}$). Rates depend strongly on the local species distribution. The highest IET rate is obtained by cell *a* in Figure 4 ($71.0 \times 10^3 \text{ e}^- \text{ s}^{-1}$), a methanogen surrounded by six acetogens, all in turn connected to fewer methanogens. The lowest rate achieved is $13.4 \times 10^3 \text{ e}^- \text{ s}^{-1}$ for cell *b* in Figure 4, one of the acetogens connected to methanogen *a*, but no other methanogens. MIET rates are not affected by the larger community (the average rate is 2% higher than for the cell pair system).

The decrease in DIET rate is due to increased activation losses and electron balancing in the network. Despite the lower average IET rate, the average activation loss per cell pair increases (from 0.38 to 0.40 mV; 93% to 97% of total voltage losses), whereas Ohmic losses is almost three times lower because of the slightly lower IET rate and many additional nanowires formed per cell (on average, $N_{nw,j} = 291$ for the multicellular system, compared with $N_{nw,j} = N_{nw,pair} = 100$ for the cell pair system).

These results suggest communities capable of DIET achieve rates lower than the cell pair system, showing that formate-MIET remains thermodynamically more favourable compared with DIET for multicellular communities using the baseline parameter set chosen. It should be emphasised, however, that DIET rates in the multicellular system can exceed the cell pair rates

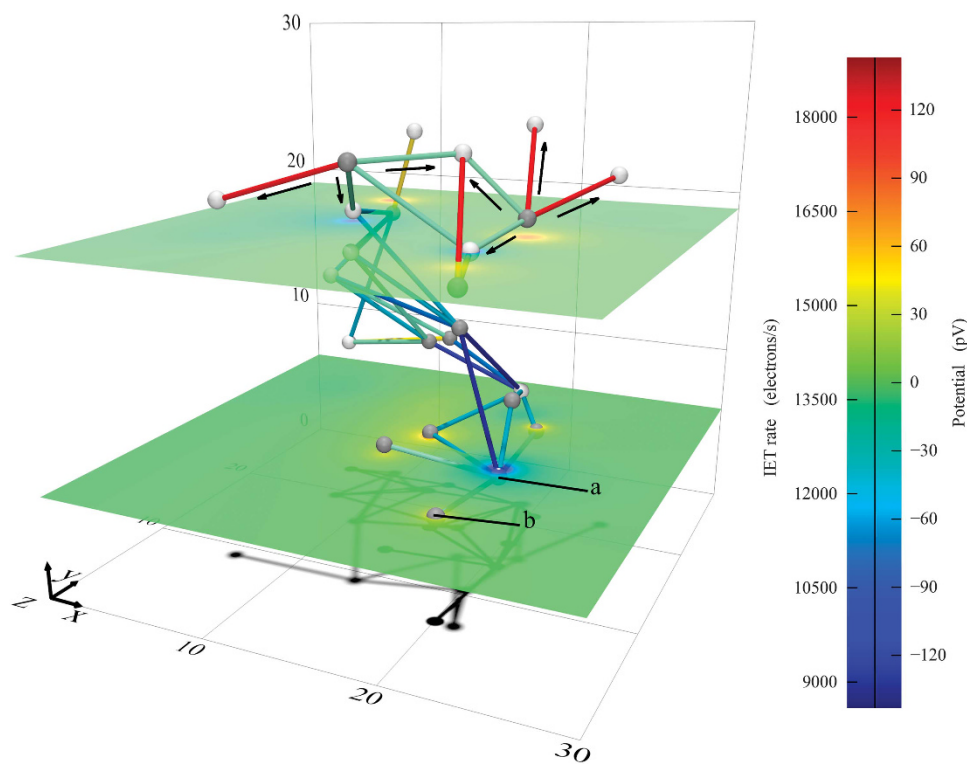


Figure 4 Cell positions (dark grey spheres are acetogens, light grey spheres methanogens), nanowires (lines, colour shows IET rate through nanowire in $\text{e}^- \text{ s}^{-1}$) and potential field because of migration (planes, colour shows potential in pV). Cell *a* achieves the highest IET rate, cell *b* the lowest. Arrows denote the direction in which electrons flow. A movie showing cell positions and potential fields from different angles is available in the Supplementary Material as Supplementary Movie 1.

if activation losses become less dominant. For example, increasing k_0 by a factor 10 (parameter set from Figure 3, case 2, simulation 3) increases the average cell IET rate to $309 \times 10^3 \text{ e}^- \text{ s}^{-1}$ (10% higher than cell pair DIET in Figure 3, case 2).

Conclusions

Investigation of extracellular losses suggests formate-MIET is thermodynamically more favourable than hydrogen-MIET (2 orders of magnitude rate difference) and DIET using nanowires (1 order of magnitude rate difference), with both MIET modes limited by diffusion flux and DIET limited by redox cofactor activation losses. In order for DIET to achieve rates comparable to or higher than formate-MIET, the true value for cell-nanowire cofactor electron transfer rate constant (k_0), cell redox cofactor concentration (c_{act}^s), area ($A_{\text{act,cell}}$) or count ($N_{\text{act,cell}}$) must be 5–10 times higher than estimated from literature published to date. Cellular metabolism may also readily compensate for a decreased favourability in external transfer feasibility (Nagarajan *et al.*, 2013) with differences on the order of less than a kJ mol^{-1} per cell compensating for electrochemical limitations in DIET.

Conflict of Interest

The authors declare no conflict of interest.

Acknowledgements

This project was supported under Australian Research Council's Discovery Projects funding scheme (project number DP0985000). Dr Bernardino Viridis is supported by strategic funding for the Centre for Microbial Electrochemical Systems (UQ). Dr Damien Batstone is the recipient of an Australian Research Fellowship.

References

- Bard A, Faulkner L. (1980). *Electrochemical Methods: Fundamentals and Applications* 2nd edn. Wiley: New York.
- Batstone DJ, Keller J, Angelidaki I, Kalyuzhnyi SV, Pavlostathis SG, Rozzi A *et al.* (2002). *Anaerobic Digestion Model No. 1*. First edit. IWA Publishing: London.
- Batstone DJ, Picioreanu C, van Loosdrecht MCM. (2006). Multidimensional modelling to investigate interspecies hydrogen transfer in anaerobic biofilm. *Water Res* **40**: 3099–3108.
- Boone DR, Bryant MP. (1980). Propionate-degrading bacterium, *Syntrophobacter wolinii* sp. nov. gen. nov., from methanogenic ecosystems. *Appl Environ Microbiol* **40**: 626–632.
- Boone DR, Johnson RL, Liu Y. (1989). Diffusion of the interspecies electron carriers H_2 and formate in methanogenic ecosystems and its implications in the measurement of km for H_2 or formate uptake. *Appl Environ Microbiol* **55**: 1735–1741.
- Bowden EF, Hawkridge FM, Chlebowski JF, Bancroft EE, Thorpe C, Blount HN. (1982). Cyclic voltammetry and derivative cyclic voltabsorptometry of purified horse heart cytochrome c at tin-doped indium oxide optically transparent electrodes. *J Am Chem Soc* **104**: 7641–7644.
- Cruz Viggì C, Rossetti S, Fazi S, Paiano P, Majone M, Aulenta F. (2014). Magnetite particles triggering a faster and more robust syntrophic pathway of methanogenic propionate degradation. *Environ Sci Technol* **48**: 7536–7543.
- Edwards MJ, Baiden NA, Johs A, Tomanicek SJ, Liang L, Shi L *et al.* (2014). The X-ray crystal structure of *Shewanella oneidensis* OmcA reveals new insight at the microbe-mineral interface. *FEBS Lett* **588**: 1886–1890.
- El-Naggar MY, Wanger G, Leung KM, Yuzvinsky TD, Southam G, Yang J *et al.* (2010). Electrical transport along bacterial nanowires from *Shewanella oneidensis* MR-1. *Proc Natl Acad Sci USA* **107**: 18127–18131.
- Gill PE, Murray W, Saunders MA. (2005). SNOPT: an SQP algorithm for large-scale constrained optimization. *SIAM Rev* **47**: 99–131.
- Hedderich R, Whitman WB. (2013). Physiology and biochemistry of the methane-producing archaea. In *The Prokaryotes*, Rosenberg E, DeLong EF, Lory S, Stackebrandt E, Thompson F (eds). Springer Berlin Heidelberg: Berlin, Heidelberg, pp 635–662.
- Heijnen JJ, Kleerebezem R. (2010). Bioenergetics of microbial growth. *Encycl Bioprocess Technol*; e-pub ahead of print 15 April 2010; doi:10.1002/9780470054581.eib084.
- Hoh CY, Cord-Ruwisch R. (1996). A practical kinetic model that considers endproduct inhibition in anaerobic digestion processes by including the equilibrium constant. *Biotechnol Bioeng* **51**: 597–604.
- Liu F, Rotaru A-E, Shrestha PM, Malvankar NS, Nevin KP, Lovley DR. (2012). Promoting direct interspecies electron transfer with activated carbon. *Energy Environ Sci* **5**: 8982–8989.
- Lovley DR. (2012). Electromicrobiology. *Annu Rev Microbiol* **66**: 391–409.
- Lower BH, Shi L, Yongsunthon R, Droubay TC, McCready DE, Lower SK. (2007). Specific bonds between an iron oxide surface and outer membrane cytochromes MtrC and OmcA from *Shewanella oneidensis* MR-1. *J Bacteriol* **189**: 4944–4952.
- Ly HK, Harnisch F, Hong S-F, Schröder U, Hildebrandt P, Millo D. (2013). Unraveling the interfacial electron transfer dynamics of electroactive microbial biofilms using surface-enhanced Raman spectroscopy. *ChemSusChem* **6**: 487–492.
- Malvankar NS, Vargas M, Nevin KP, Franks AE, Leang C, Kim B-C *et al.* (2011). Tunable metallic-like conductivity in microbial nanowire networks. *Nat Nanotechnol* **6**: 573–579.
- Malvankar NS, Yalcin SE, Tuominen MT, Lovley DR. (2014). Visualization of charge propagation along individual pili proteins using ambient electrostatic force microscopy. *Nat Nanotechnol* **9**: 1012–1017.
- Mehta T, Coppi MV, Childers SE, Lovley DR. (2005). Outer membrane c-type cytochromes required for Fe(III) and Mn(IV) oxide reduction in *Geobacter sulfurreducens*. *Appl Environ Microbiol* **71**: 8634–8641.
- Morita M, Malvankar NS, Franks AE, Summers ZM, Giloteaux L, Rotaru A-E *et al.* (2011). Potential for direct interspecies electron transfer in methanogenic wastewater digester aggregates. *MBio* **2**: e00159–11.

- Nagarajan H, Embree M, Rotaru A-E, Shrestha PM, Feist AM, Palsson BØ *et al.* (2013). Characterization and modelling of interspecies electron transfer mechanisms and microbial community dynamics of a syntrophic association. *Nat Commun* **4**: 2809.
- Noren DA, Hoffman MA. (2005). Clarifying the Butler–Volmer equation and related approximations for calculating activation losses in solid oxide fuel cell models. *J Power Sources* **152**: 175–181.
- Okamoto A, Nakamura R, Hashimoto K. (2011). *In-vivo* identification of direct electron transfer from *Shewanella oneidensis* MR-1 to electrodes via outer-membrane OmcA–MtrCAB protein complexes. *Electrochim Acta* **56**: 5526–5531.
- Okamoto A, Nakamura R, Ishii K, Hashimoto K. (2009). *In vivo* electrochemistry of C-type cytochrome-mediated electron-transfer with chemical marking. *Chembiochem* **10**: 2329–2332.
- Pirbadian S, Barchinger SE, Leung KM, Byun HS, Jangir Y, Bouhenni Ra *et al.* (2014). *Shewanella oneidensis* MR-1 nanowires are outer membrane and periplasmic extensions of the extracellular electron transport components. *Proc Natl Acad Sci* **111**: 12883–12888.
- Reed DE, Hawkrige FM. (1987). Direct electron transfer reactions of cytochrome c at silver electrodes. *Anal Chem* **59**: 2334–2339.
- Rotaru A-E, Shrestha PM, Liu F, Markovaite B, Chen S, Nevin K *et al.* (2014a). Direct interspecies electron transfer between *Geobacter metallireducens* and *Methanosarcina barkeri*. *Appl Environ Microbiol* **80**: 4599–4605.
- Rotaru A-E, Shrestha PM, Liu F, Shrestha M, Shrestha D, Embree M *et al.* (2014b). A new model for electron flow during anaerobic digestion: direct interspecies electron transfer to Methanosaeta for the reduction of carbon dioxide to methane. *Energy Environ Sci* **7**: 408–415.
- Shi L, Richardson DJ, Wang Z, Kerisit SN, Rosso KM, Zachara JM *et al.* (2009). The roles of outer membrane cytochromes of *Shewanella* and *Geobacter* in extracellular electron transfer. *Environ Microbiol Rep* **1**: 220–227.
- Shrestha PM, Rotaru A-E, Aklujkar M, Liu F, Shrestha M, Summers ZM *et al.* (2013). Syntrophic growth with direct interspecies electron transfer as the primary mechanism for energy exchange. *Environ Microbiol Rep* **5**: 904–910.
- Stams AJM, De Bok FAM, Plugge CM, van Eekert MHA, Dolging J, Schraa G. (2006). Exocellular electron transfer in anaerobic microbial communities. *Environ Microbiol* **8**: 371–382.
- Stams AJM, Plugge CM. (2009). Electron transfer in syntrophic communities of anaerobic bacteria and archaea. *Nat Rev Micro* **7**: 568–577.
- Summers ZM, Fogarty HE, Leang C, Franks AE, Malvankar NS, Lovley DR. (2010). Direct exchange of electrons within aggregates of an evolved syntrophic coculture of anaerobic bacteria. *Science* **330**: 1413–1415.
- Vargas M, Malvankar NS, Tremblay P-L, Leang C, Smith JA, Patel P *et al.* (2013). Aromatic amino acids required for pili conductivity and long-range extracellular electron transport in *Geobacter sulfurreducens*. *MBio* **4**: e00105–e00113.
- Wigginton NS, Rosso KM, Lower BH, Shi L, Hochella MF. (2007). Electrons tunneling properties of outer-membrane decaheme cytochromes from *Shewanella oneidensis*. *Geochim Cosmochim Acta* **71**: 543–555.

Supplementary Information accompanies this paper on The ISME Journal website (<http://www.nature.com/ismej>)